Assembly of Multiple DNA Components through Target Binding toward Homogeneous, Isothermally Amplified, and Specific Detection of Proteins

ARTICLE *in* ANALYTICAL CHEMISTRY · JUNE 2014

Impact Factor: 5.64 · DOI: 10.1021/ac5011316 · Source: PubMed

3 AUTHORS, INCLUDING:

Bin Deng
York University
15 PUBLICATIONS **65** CITATIONS
SEE PROFILE

Hongquan Zhang
University of Alberta
35 PUBLICATIONS **1,192** CITATIONS
SEE PROFILE

analytical chemistry

Article

pubs.acs.org/ac

Assembly of Multiple DNA Components through Target Binding toward Homogeneous, Isothermally Amplified, and Specific Detection of Proteins

Bin Deng,[†] Junbo Chen,[†,‡] and Hongquan Zhang*[,†]

[†]Department of Laboratory Medicine and Pathology, Faculty of Medicine and Dentistry, University of Alberta, 10-102 Clinical Sciences Building, Edmonton, Alberta T6G 2G3, Canada

[‡]Analytical & Testing Center, Sichuan University, Chengdu, Sichuan 610064, China

Supporting Information

ABSTRACT: We describe a strategy of utilizing specific target binding to trigger assembly of three DNA components that are otherwise unable to spontaneously assemble with one another. This binding-induced DNA assembly forms a three-arm DNA junction, subsequently initiating nicking endonuclease-assisted isothermal fluorescence signal amplification. Real-time monitoring of fluorescence enables amplified detection of specific protein targets. The implementation of the strategy necessitates the simultaneous binding of a single target molecule with two affinity ligands each conjugated to a DNA motif. Simple alternation of affinity ligands enables different protein targets to induce the formation of the DNA junction and subsequent isothermal amplification. The use of the strategy allowed us to develop a sensitive assay for proteins with three appealing features: homogeneous analysis without the need for separation, isothermal amplification, and high specificity. Streptavidin was chosen as an initial target to establish and optimize the assay. Sensitivity of protein detection was improved by 1000-fold upon the application of isothermal amplification. A limit of detection of 10 pM was achieved for detection of prostate-specific antigen in buffer and diluted serum. The combination of its three appealing features makes the assay attractive for potential applications in molecular diagnosis, point-of-care testing, and on-site analysis.

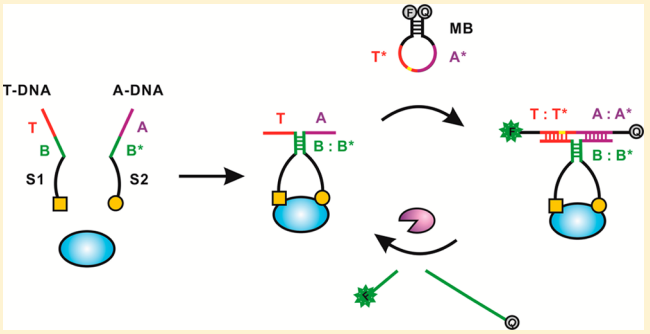

Central to structural DNA nanotechnology are DNA self-assembly and branched DNA molecules.[1−5] Self-assembly of branched DNA molecules allows for the construction of two- and three-dimensional DNA structures. Thanks to exquisite specificity, favorable predictability, and combinatorial diversity of DNA hybridization, it is feasible to design and fabricate branched DNA molecules containing three, four, or more arms.[6−10] To form a branched DNA molecule having a specific number of arms, self-association of the same number of DNA strands is implemented, creating hybridization of each strand with two other strands. Three- and four-arm DNA junctions are typically used to achieve bottom-up construction of nanostructures of varying sizes and complexity.[11−16]

Additionally, three- or four-arm DNA junctions have been used as probes for amplified detection of nucleic acids.[17−23] Junction probes function via a so-called template-enhanced hybridization process, which can be depicted by using a three-arm junction probe.[17,18] The three strands that form the three-arm DNA junction are designated as target DNA, assistant DNA, and reporter DNA dually labeled with a reporter dye and a quenching molecule. The presence of target DNA leads to formation of a three-arm junction, enabling hybridization between the reporter DNA and the assistant DNA, which is otherwise unstable in the absence of the target DNA. The formation of the junction probe initiates the cycling enzymatic cleavage of the reporter DNA, achieving amplified detection.

We recently proposed a new concept of DNA assembly termed binding-induced DNA assembly (BINDA).[24,25] Distinct from DNA self-assembly, DNA components for BINDA cannot spontaneously assemble with one another and can assemble together only when a specific target triggers a binding event. Because it relies upon target binding, BINDA is an excellent strategy to convert binding of proteins and other biomolecules into detection of amplifiable DNA. Based on BINDA, we have developed several homogeneous protein assays, involving assembly of two DNA components through target binding.[26−31] These assays allow nonamplified or exponentially amplified detection of proteins through adaptation of enzyme-free fluorescence detection or real-time PCR into detection of BINDA. The use of BINDA to achieve homogeneous and isothermally amplified protein detection has not been demonstrated. Isothermally amplified detection of proteins in a mix-and-read approach is attractive for potential applications

Received: March 28, 2014
Accepted: June 19, 2014
Published: June 19, 2014

   dx.doi.org/10.1021/ac5011316 | *Anal. Chem.* 2014, 86, 7009−7016

Scheme 1. Schematic Showing the Principle of Homogeneous, Isothermal, and Amplified Detection of Proteins through Binding-Induced Assembly of Three DNA Components[a]

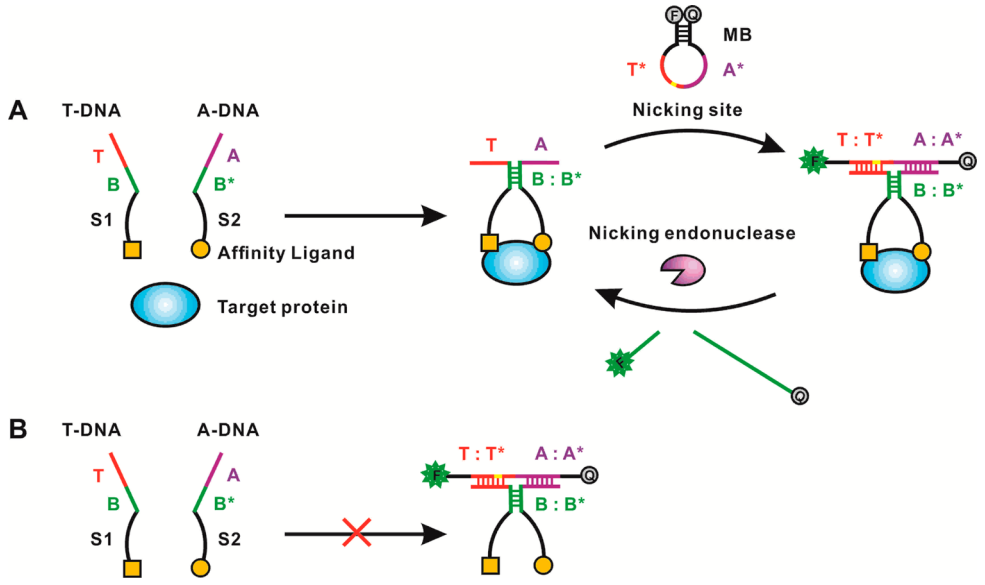

[a](A) The binding of two affinity ligands to the same target molecule confines T-DNA and A-DNA within a ternary complex molecule, thereby inducing hybridization of **B** and **B***. As a consequence, **T** is placed adjacent to **A**, which leads to the assembly of T-DNA, A-DNA, and MB through cooperative hybridization of **T** and **A** with **T*** and **A***, forming a three-arm DNA junction. The formation of the DNA junction triggers NEase-assisted cycling cleavage of MB, enabling isothermal and amplified detection of proteins. (B) In the absence of protein targets, T-DNA, A-DNA, and MB cannot assemble into a DNA junction, and therefore no enzymatic cleavage of MB occurs.

in point-of-care testing and on-site analysis because thermal cycling is not required to achieve amplification. The objective of this study is to develop a sensitive assay for proteins with three appealing features: homogeneous analysis without the need for separation, isothermal amplification, and high specificity. To achieve this, we describe herein a strategy to assemble three DNA components via specific target binding, forming a binding-induced three-arm DNA junction. The formation of the DNA junction initiates enzymatic fluorescence signal amplification, enabling homogeneous and isothermally amplified detection of proteins.

EXPERIMENTAL SECTION

Materials and Reagents. All DNA oligonucleotides were synthesized, labeled, and purified by Integrated DNA Technologies (IDT, Coralville, IA). The DNA sequences and modifications are listed in Table S1 and Figure S1 of the Supporting Information. Biotin, streptavidin, bovine serum albumin (BSA), prostate-specific antigen (PSA), and human serum were purchased from Sigma-Aldrich (Oakville, ON). Biotinylated polyclonal anti-PSA antibody was obtained from R&D Systems (Minneapolis, MN). Nicking endonucleases (NEases), Nt.BsmAI and Nt.BbvCI, and 10× NEB buffer (500 mM potassium acetate, 200 mM Tris-acetate, 100 mM magnesium acetate, 10 mM dithiothreitol, pH 7.9) were obtained from New England BioLabs (Whitby, ON). Phosphate-buffered saline (1× PBS) (137 mM NaCl, 10 mM phosphate, 2.7 mM KCl, pH 7.4) was diluted with deionized water from 10× PBS buffer (Fisher Scientific, Nepean, ON). All other reagents were of analytical grade.

Experimental Optimization of the Assay Using Streptavidin as a Target. Streptavidin was used as an initial target to optimize the key parameters of the assay, including length of complementary sequences (**T** and **T***, **A** and **A***, and **B** and **B***), concentration of trigger DNA (T-DNA) and assistant DNA (A-DNA), stability of the molecular beacon (MB), blocking DNA, and NEases. The aim of the optimization was to obtain the largest signal-to-background ratio. Optimization of a specific parameter was carried out by analysis of a series of sample and blank solutions, where other conditions were kept unaltered except the parameter being optimized. Sample solutions were prepared to contain 200 pM streptavidin in 100 μL of 1× NEB buffer containing 0.1% BSA, and blank solutions contained all other ingredients except streptavidin. After incubation of sample and blank solutions at room temperature for 30 min, 10 units of NEase were added into each solution. The solutions were then loaded into a multimode microplate reader (DX800, Beckman Coulter) set with a temperature of 37 °C for real-time monitoring of fluorescence. The fluorescence was measured at every 5 min for 2 h by using 485 nm for excitation and 515 nm for emission. Analyses were carried out in duplicate. The fluorescence values of sample and blank solutions at the 2 h amplification end points were used to calculate the signal-to-background ratio. We subtracted from each fluorescence value the background fluorescence of the molecular beacon due to incomplete quenching in order to address the background resulting from target-independent DNA assembly.

The optimum conditions were further applied to analysis of solutions containing varying concentrations of streptavidin. The solutions were prepared to contain varying concentrations of streptavidin, 100 nM MB1, 1 nM T-DNA containing **B** of 7 bases, 1 nM A-DNA containing **A** of 7 bases, and 200 nM blocking DNA containing 10 bases in 100 μL of 1× NEB with 0.1% BSA. After incubation of solutions at room temperature for 30 min, 10 units of Nt.BsmAI were added into each solution. The solutions were then loaded into the multimode

dx.doi.org/10.1021/ac5011316 | Anal. Chem. 2014, 86, 7009−7016

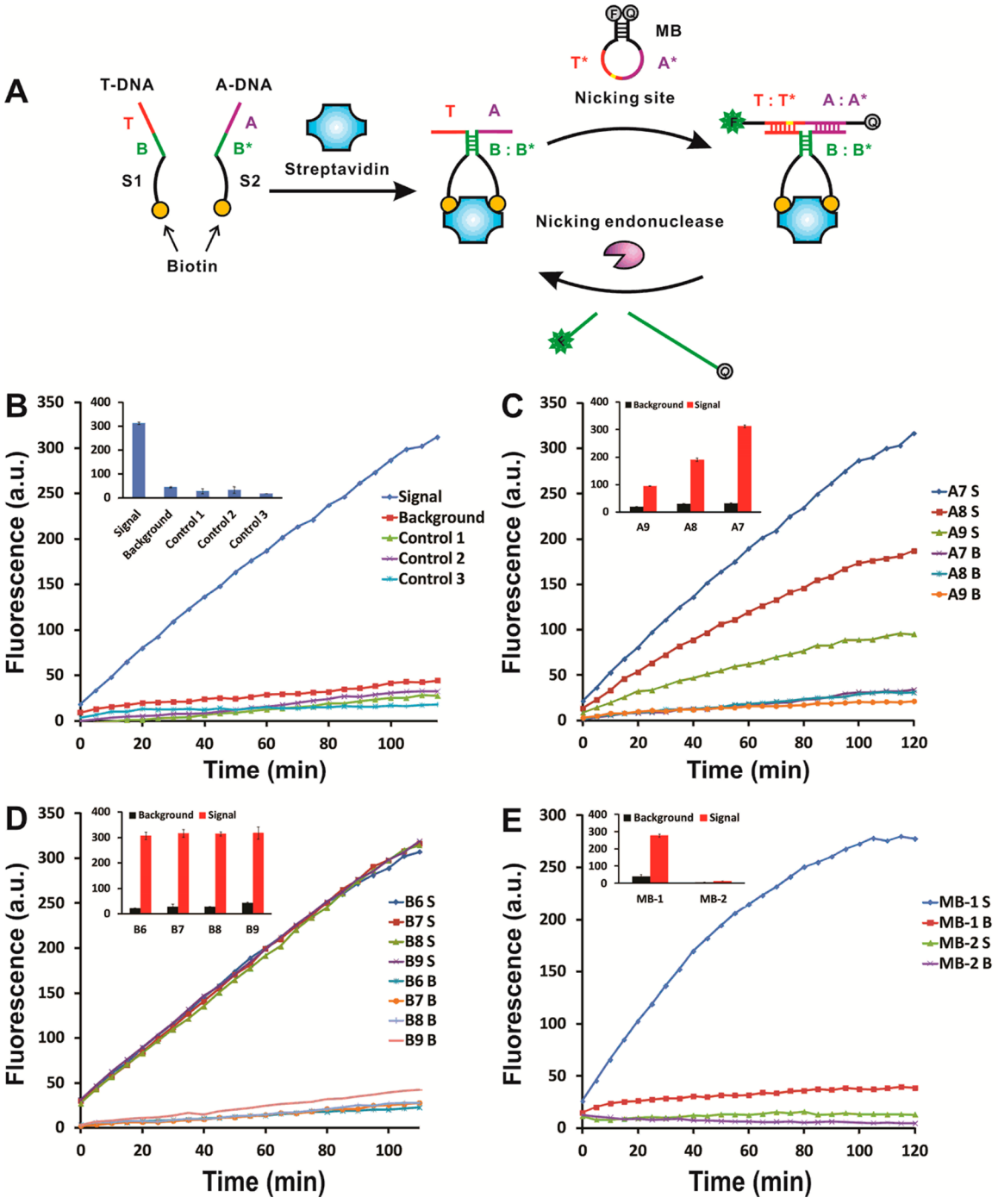

Figure 1. Establishment and optimization of the assay using streptavidin as a target. (A) Schematic showing amplified detection of streptavidin. (B) Amplification curves from analysis of a sample containing 200 pM streptavidin, a blank containing all other ingredients except streptavidin, control 1 and 2 containing 200 pM streptavidin only bound with T-DNA or A-DNA, respectively, and control 3 containing 100 nM MB and 1 nM T-DNA. (C) Impact of the length of **A** on signal and background. (D) Impact of the length of **B** on signal and background. (E) Comparison of performances of two MBs with different stability. Inset figures show the signal and background values of the 2 h amplification end points. In figures C, D, and E, "S" means signal and "B" means background.

microplate reader set at 37 °C for real-time monitoring of fluorescence.

Detection of Prostate-Specific Antigen. To detect PSA, biotinylated polyclonal anti-PSA antibodies were linked with T-DNA or A-DNA through biotin−streptavidin interaction. Specifically, 100 μL of 800 nM biotinylated T-DNA or A-DNA was mixed with 100 μL of 800 nM streptavidin in PBS buffer containing 0.1% BSA. After incubation of the two mixtures at room temperature for 1 h, 200 μL of 400 nM biotinylated anti-PSA antibodies was added to each mixture. The mixtures were incubated at room temperature for 30 min to form antibody-conjugated T-DNA or A-DNA. The DNA solutions were further diluted to 100 nM in PBS buffer containing 0.1% BSA and 10 μM biotin. The excess amount of biotin was used to occupy the free biotin-binding sites of

dx.doi.org/10.1021/ac5011316 | Anal. Chem. 2014, 86, 7009−7016

streptavidin. The probe solutions were stored at 4 °C prior to use.

PSA was measured in 1× NEB buffer and in diluted serum. Varying concentrations of PSA were prepared in 100 μL of 1× NEB buffer or of 5% human serum in 1× NEB buffer containing 100 nM MB1, 1 nM antibody-conjugated T-DNA and A-DNA, and 200 nM blocking DNA. The solutions were incubated at 37 °C for 30 min, allowing the binding of antibodies to PSA molecules. Ten units of Nt.BsmAI were then added to each solution. The solutions were then loaded into the microplate reader set with a temperature of 37 °C for real-time monitoring of fluorescence. The fluorescence was measured in real time at 5 min intervals for 2 h by using 485 nm for excitation and 515 nm for emission. Analyses were carried out in duplicate. The fluorescence values of the 2 h amplification end points were used to establish calibration curves.

RESULTS AND DISCUSSION

Design Principle of the Assay. The aim of the strategy is to accomplish the assembly of three DNA components upon the specific target binding and yet eliminate their self-assembly in the absence of protein targets. To achieve this, we designed three DNA strands, a trigger DNA (T-DNA), an assistant DNA (A-DNA), and a molecular beacon (MB) as a signal DNA (Scheme 1). T-DNA and A-DNA are each conjugated to an affinity ligand recognizing the target molecule. T-DNA and A-DNA are designed to each comprise three domains: **S1**, **B**, and **T**, and **S2**, **B***, and **A**, respectively. **S1** and **S2** are used to render spatial distance, facilitating detection of protein molecules of varying sizes. **B** is complementary to **B***, and **T** and **A** are complementary to loop domains **T*** and **A*** of MB, respectively. To obviate target-independent assembly of three DNA strands, complementary sequences are designed to only contain 6−9 nucleotides so that their hybrids are unstable at ambient temperature. In the presence of the protein targets, the binding of two affinity ligands to the same target molecule confines T-DNA and A-DNA within a ternary complex molecule, dramatically increasing the local effective concentration of **B** and **B***. As a result, the stability of hybrid between **B** and **B*** is largely enhanced, enabling their hybridization. The hybridization of **B** and **B*** places **T** adjacent to **A**, thereby facilitating their cooperative hybridization with the loop of MB, which consequently leads to formation of a three-arm DNA junction, disrupting the stem-loop structure of MB and restoring fluorescence. Meanwhile, the hybridization between **T** and **T*** forms a complete recognition sequence of a NEase, initiating the enzymatic cleavage of the loop of MB and releasing the ternary complex for hybridization with another MB. Cycling enzymatic cleavage is therefore accomplished along with fluorescence increase. The real-time monitoring of fluorescence enables amplified detection of protein targets. The whole analysis can be carried out at 37 °C in a single tube without the need for separation.

Establishment of the Assay Using Streptavidin as a Target. To demonstrate the proof of the concept, we chose streptavidin as the initial target because its extraordinary binding affinity to biotin facilitates the establishment of the assay. To detect streptavidin, T-DNA and A-DNA were each conjugated with a biotin molecule (Figure 1A). The binding of two biotin molecules to the same streptavidin molecule induces the hybridization of **B** and **B***, bringing **T** adjacent to **A**. Because there are four biotin-binding sites in each streptavidin molecule, T-DNA and A-DNA can bind with one streptavidin molecule at sites adjacent (ortho-style) or opposite (para-style) each other. The scheme in Figure 1A shows binding of T-DNA and A-DNA with a streptavidin molecule in ortho-style. Consequently, assembly of T-DNA, A-DNA, and MB is realized through cooperative hybridization of **T** and **A** with **T*** and **A***, forming a three-arm DNA junction. The formation of the DNA junction triggers the cycling enzymatic cleavage of MB, leading to amplified detection of streptavidin. When the assay was applied to analysis of a sample containing 200 pM streptavidin, steady increase in fluorescence signal was attained with increasing amplification time, proving the formation of the DNA junction and the consequent enzymatic amplification (Figure 1B). In contrast, little fluorescence increase resulted from a blank containing all other ingredients except streptavidin. The fluorescence values of 2 h amplification end points were used for quantitation of streptavidin, because the largest fluorescence increase was obtained at the end points of the amplification.

The binding of two affinity molecules to the same target molecule is requisite for the assay to generate detection signal. To demonstrate this, we first introduced T-DNA or A-DNA to bind to streptavidin, followed by adding the excess amount of biotin molecules to occupy the free biotin-binding sites. Therefore, each streptavidin molecule was only bound by one DNA strand. Little fluorescence increase was observed for these instances, proving the necessity of simultaneous binding of two affinity molecules to a single target molecule (Figure 1B). The requirement of the two simultaneous binding events enhances the specificity of the assay.

The sensitivity of the assay relies on accomplishing the assembly of T-DNA, A-DNA, and MB upon the target binding while minimizing the target-independent assembly. Three pairs of complementary sequences (**T** and **T***, **A** and **A***, and **B** and **B***) were designed to secure binding-induced assembly of three DNA strands that leads to a detection signal and to obviate their self-assembly that results in background. In order to attain the largest signal-to-background ratio, we studied the impact of these complementary sequences on analysis. We designed three A-DNA and four T-DNA, creating three different sequences for **A** and four different sequences for **B** (Figure S1A of the Supporting Information). The complementary pair **T** and **T*** is committed to contain the recognition sequence of a NEase, Nt.Bsm.AI, and self-hybridization between **T** and **T*** can directly generate background. We therefore designed **T** and **T*** to have minimal bases (eight nucleotides) that are essential to the activity of Nt.Bsm.AI. No fluorescence increase was observed for the control containing 100 nM MB and 1 nM T-DNA, suggesting that self-hybridization between **T** and **T*** was eliminated (Figure 1B).

We then used the T-DNA containing seven bases for **B** to examine the performances of three A-DNA containing eight and nine bases for **A** (**A7**, **A8**, and **A9**), respectively. As shown in Figure 1C, shorter **A** led to larger fluorescence increase over the amplification time, which suggests that the length of **A** can impact the amplification rate of the analysis. Shorter **A** facilitates release of the ternary complex from the cleaved MB, thereby shortening the time required for each cleavage cycle. As a result, **A7** resulted in the fastest amplification rate. A slight increase in background was observed for all three DNA, and **A9** showed the lowest background, which can be understood by its slowest amplification rate. The **A7** rendered the largest signal-to-background ratio. We therefore used the A-DNA with **A7** to compare the four T-DNA containing six to

dx.doi.org/10.1021/ac5011316 | Anal. Chem. 2014, 86, 7009−7016

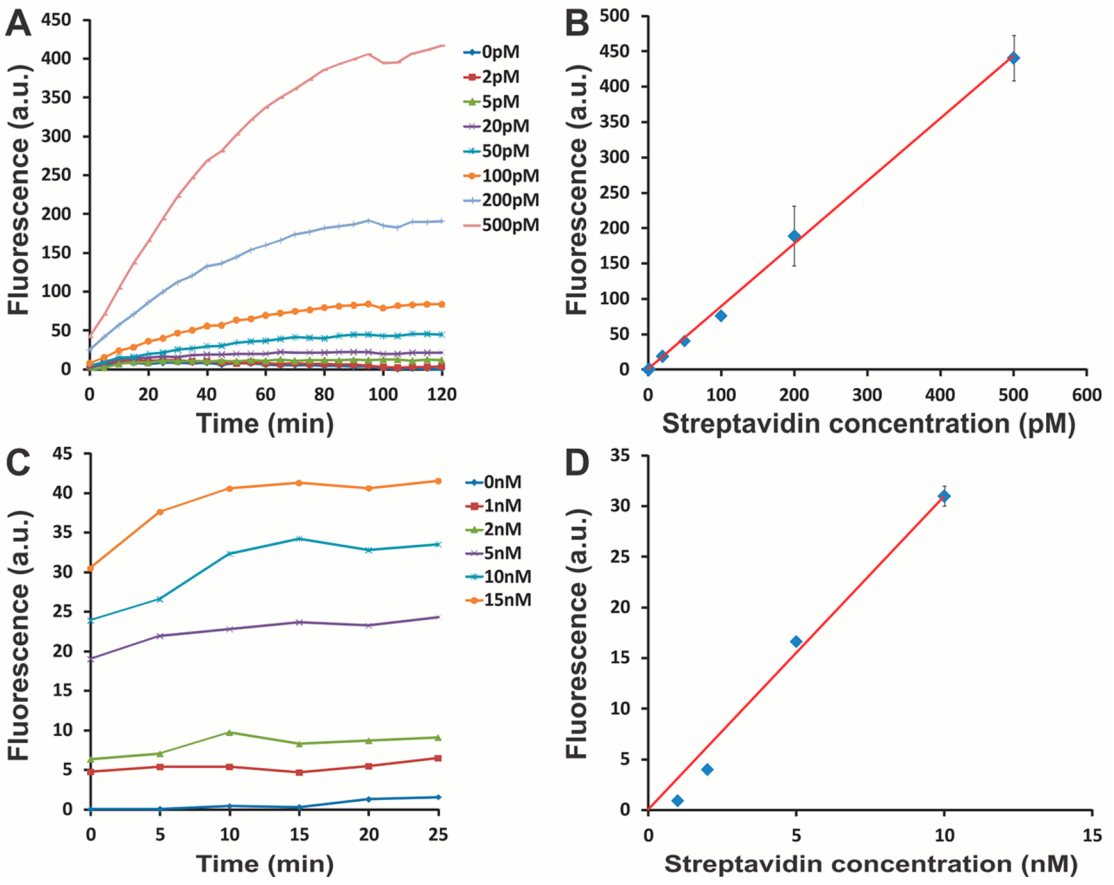

Figure 2. Analysis of varying concentrations of streptavidin. (A) NEase-assisted amplification curves from analysis of streptavidin at varying concentrations. (B) Calibration curve of the assay using fluorescence values of the 2 h amplification end points. (C) Fluorescence changes over the detection time for streptavidin analysis without the use of NEase. (D) Calibration curve of streptavidin analysis without the use of NEase.

nine bases for **B** (**B6**, **B7**, **B8**, **B9**), which allowed us to study the impact of the length of **B** on the analysis. No obvious difference in fluorescence signal increase was observed for all four T-DNA, suggesting that the length of **B** has little impact on the amplification rate of the analysis (Figure 1D). Little increase in background was observed for **B** having six to eight bases. However, **B9** led to a larger increase in background, suggesting the use of longer **B** can increase the incidence of target-independent DNA assembly. Similar signal-to-background ratios were obtained for **B6**, **B7**, and **B8**. It should be noted that in addition to their length, the sequence composition of these complementary pairs also gives rise to impacts on the analysis. For two complementary sequences with a specific length, increasing guanine−cytosine content improves the stability of hybrid of the two sequences. Free energy (ΔG) is a parameter that can be used to comprehensively indicate the impacts of both sequence length and composition. The estimated ΔG values of tested complementary sequences (**A** and **A***, **B** and **B***, and **T** and **T***) are listed in Table S2. The extension of the length of complementary sequences reduces the ΔG value. The lower ΔG value means higher stability for a DNA duplex.

We also examined the impact of the concentrations of T-DNA and A-DNA on background because the incidence of target-independent DNA assembly is directly associated with DNA concentrations. The background became larger with the increase of DNA concentration from 0.5 nM to 10 nM, and the largest signal-to-background ratio was obtained for 1 nM of T-DNA and A-DNA (Figure S2 of the Supporting Information). In order to further reduce the background resulting from target-independent DNA assembly, we designed a blocking DNA that is complementary to a portion of **B** and **T** (Figure S1B of the Supporting Information). Therefore, the blocking DNA competes with A-DNA and MB in hybridization with T-DNA. We compared three blocking DNA having 10 to 12 bases. The use of blocking DNA effectively reduced the background. However, the longer blocking DNA compromised the fluorescence signal. The blocking DNA of 10 bases gave rise to the best signal-to-background ratio (Figure S3 of the Supporting Information). We also studied the impact of the MB concentration on analysis. A concentration of 100 nM MB showed satisfactory results in both fluorescence signal intensity and signal-to-background ratio (Figure S4 of the Supporting Information).

As illustrated in Scheme 1, each enzymatic cleavage cycle encompasses the separation of the MB stem and the formation of the DNA junction. Therefore, if MB is too stable to be disrupted, the formation of the DNA junction becomes difficult, reducing the amplification efficiency. On the other hand, MB needs to be sufficiently stable at the amplification temperature (37 °C), so that low background fluorescence results from incomplete fluorescence quenching of MB. We designed two MBs with different stability. The melting temperature is 43.8 °C for the MB1 and 59.0 °C for the MB2, which was estimated by IDT OligoAnalyzer under conditions of 50 mM NaCl and 10 mM $MgCl_2$. Therefore, both MBs are stable at 37 °C. In

dx.doi.org/10.1021/ac5011316 | *Anal. Chem.* 2014, 86, 7009−7016

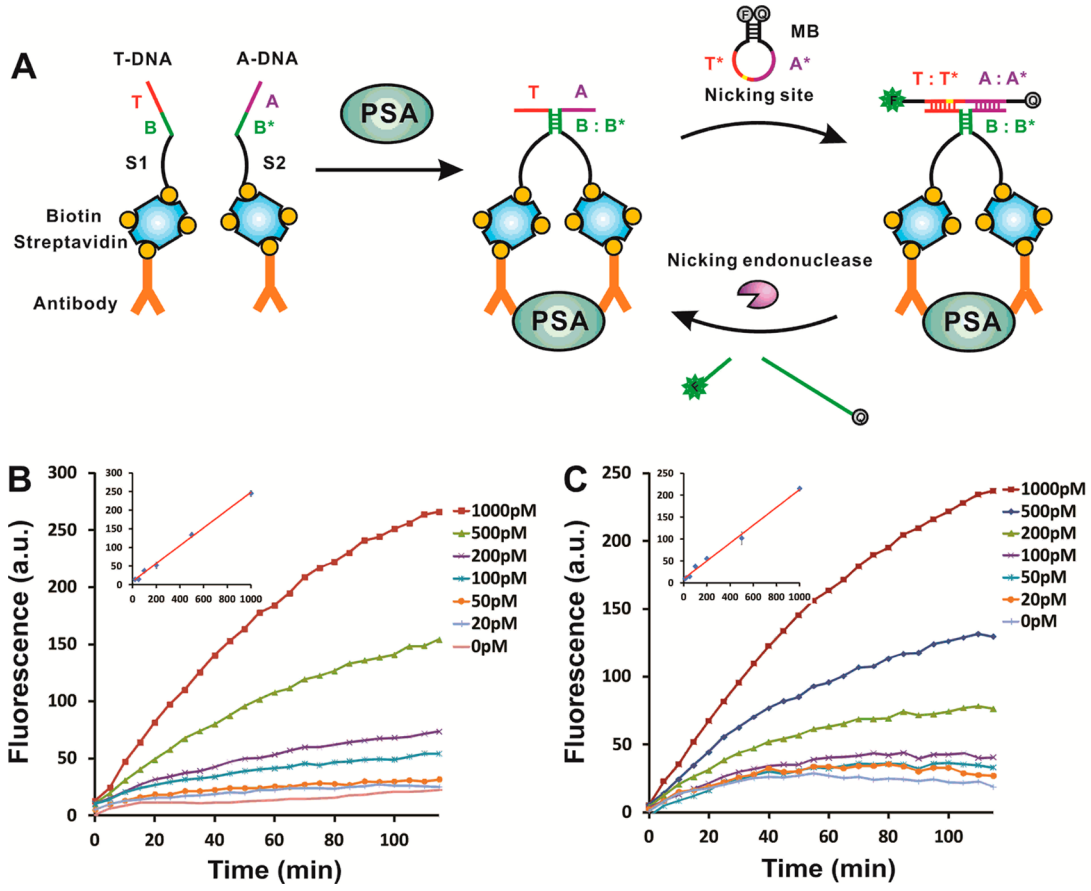

Figure 3. Analysis of PSA in 1× NEB buffer and in diluted serum. (A) Schematic showing amplified detection of PSA. (B) Amplification curves from analysis of varying concentrations of PSA in 1× NEB buffer. (C) Amplification curves from analysis of varying concentrations of PSA in diluted serum. Inset figures show calibration curves using fluorescence values of the 2 h amplification end points.

addition, an unpaired T base and A base were added between **T*** and **A***, for MB1, which can thermodynamically improve the formation of the DNA junction. Figure 1E shows that the stability of MB largely impacted signal amplification and the sensitivity of analysis. The less stable MB1 resulted in much larger fluorescence signal than the more stable MB2. When T-DNA and A-DNA containing longer **B** and **A** were used to enhance the separation of MB stem, no large increase in fluorescence was observed for the use of MB2 (Figure S5 of the Supporting Information). **A** and **A*** were also designed to contain a recognition sequence for a second NEase (Nt.BbvCI) in order to compare the behavior of two different enzymes. No fluorescence increase was observed from 1× NEB buffer containing 200 pM streptavidin when Nt.BbvCI was used, whereas the use of Nt.Bsm.AI led to a large fluorescence increase (Figure S6 of the Supporting Information). In order to determine the potential reasons, we tested the activity of Nt.BbvCI for analyzing a mixture of 100 nM MB1 and 1 nM A-DNA-A9 containing nine bases of A (Table S1). A clear fluorescence increase was observed, which suggested that Nt.BbvCI was active for the cleavage of MB1 when a double DNA duplex is formed upon the hybridization of MB1 with A-DNA-A9. Therefore, Nt.BbvCI is active for cleavage of its recognition sequence in the double DNA duplex, but not for that in the three-arm DNA junction, which is probably because the recognition sequence is adjacent to the junction point in the DNA junction structure, disabling the interaction of Nt.BbvCI with its recognition sequence.

We then applied the assay to analysis of solutions containing varying concentrations of streptavidin (Figure 2). The fluorescence increase is proportional to streptavidin concentration. A linear dynamic range was obtained from 2 pM to 500 pM. A detection limit, defined as the concentration equivalent to three times the standard deviation of the background, was 1 pM. To determine the sensitivity improvement resulting from NEase-assisted amplification, we carried out the streptavidin analysis without the use of NEase. No fluorescence increase was observed over the detection time. A detection limit of 1 nM was obtained, indicating that the sensitivity of analysis was improved by 1000-fold upon the application of NEase-assisted amplification.

Assay for Prostate-Specific Antigen. The optimized assay from streptavidin analysis can be readily generalized to analysis of other protein targets by simply incorporating the corresponding affinity ligands to T-DNA and A-DNA because of two main reasons: (1) the optimized three DNA components (T-DNA, A-DNA, and MB) enabled the minimization of the background resulting from target-independent assembly, which is equally effective for the incorporation of different affinity ligands; (2) **S1** and **S2** were designed to render sufficient spatial distance, thereby allowing the binding of target molecules of different sizes to induce the assembly of three DNA components. To accommodate molecules of different sizes, we designed the length of **S1** and **S2** to contain 66 nucleotides, which is equivalent to a maximum length of ~22 nm (based on 3.3 Å per nucleotide).[25] This

dx.doi.org/10.1021/ac5011316 | *Anal. Chem.* 2014, 86, 7009−7016

length is larger than diameters of most protein molecules. To demonstrate the applicability of the assay, we used it to detect PSA in buffer and serum matrices. To detect PSA, biotinylated polyclonal anti-PSA antibodies were linked with T-DNA or A-DNA using streptavidin as the connecting molecule (Figure 3A). We first mixed T-DNA or A-DNA with streptavidin at a 1:1 molar ratio, allowing one DNA strand to bind with a single streptavidin molecule. The same molar amount of biotinylated antibody was then added into the mixture. As a consequence, one DNA strand is linked to one antibody molecule through a streptavidin molecule. Because there are three free biotin-binding sites in each streptavidin molecule for biotinylated antibody binding, the antibody can be attached to the biotin binding site adjacent (ortho-style) or opposite (para-style) to the DNA strand. The scheme in Figure 3A shows DNA–antibody conjugates in para-style.

Figure 3B shows the detection of PSA in 1× NEB buffer. The fluorescence increase is concentration-dependent, and higher concentration of PSA led to faster fluorescence increase. A linear dynamic range was obtained from 20 pM to 1000 pM when fluorescence values of the 2 h amplification end points were used for quantitation. A detection limit of 10 pM was attained, which is below the clinical diagnostic cutoff. We also examined the specificity of the assay by applying it to detection of four other proteins (human immunoglobulin, transferrin, human serum albumin, and thrombin). Compared to the blank, no fluorescence increase can be clearly observed for 10 nM in these four proteins, whereas 1 nM PSA led to a large fluorescence increase (Figure S7 of the Supporting Information), which suggests that the specificity of assay is high. The high specificity of the assay is largely attributed to the requirement of two binding events for a single target molecule. We further detected PSA in 20× diluted serum samples. The similar linear dymanic range and detection limit were achieved, suggesting that the serum matrix did not greatly interfere with the PSA analysis (Figure 3C).

CONCLUSIONS

We have demonstrated the use of specific target binding to trigger assembly of three DNA components that are otherwise unable to spontaneously assemble with one another. The capability to assemble three DNA components upon the target binding allowed us to develop a homogeneous, isothermal amplification assay for proteins. The assay can be conducted in a single tube without the need for separation. The NEase-assisted isothermal amplification improved the sensitivity of protein detection by 1000-fold. The assay exhibits high specificity, taking advantage of the requirement of two simultaneous binding events for a single target molecule. Additionally, the assay can be readily extended to other biological molecules by simple incorporation of the corresponding binding molecules. The combination of these advantages makes the assay attractive for potential applications in molecular diagnosis, point-of-care testing, and on-site analysis.

ASSOCIATED CONTENT

Supporting Information

Additional information as noted in the text (Tables S1 and S2, Figures S1–S7). This material is available free of charge via the Internet at http://pubs.acs.org.

AUTHOR INFORMATION

Corresponding Author

*E-mail: hongquan@ualberta.ca.

Notes

The authors declare no competing financial interest.

ACKNOWLEDGMENTS

The authors acknowledge the financial support from the Natural Sciences and Engineering Research Council of Canada, the University Hospital Foundation, University of Alberta, and Alberta Health.

REFERENCES

(1) Seeman, N. C. *Nature* **2003**, *421*, 427–431.
(2) Aldaye, F. A.; Palmer, A. L.; Sleiman, H. F. *Science* **2008**, *321*, 1795–1799.
(3) Seeman, N. C. *Annu. Rev. Biochem.* **2010**, *79*, 65–87.
(4) Dietz, H.; Douglas, S. M.; Shih, W. M. *Science* **2009**, *325*, 725–730.
(5) Douglas, S. M.; Dietz, H.; Liedl, T.; Högberg, B.; Graf, F.; Shih, W. M. *Nature* **2009**, *459*, 414–418.
(6) Seeman, N. C. *J. Theor. Biol.* **1982**, *99*, 237–247.
(7) Ma, R.-I.; Kallenbach, N. R.; Sheardy, R. D.; Petrillo, M. L.; Seeman, N. C. *Nucleic Acids Res.* **1986**, *14*, 9754–9753.
(8) Yang, H.; Sleiman, H. F. *Angew. Chem., Int. Ed.* **2008**, *47*, 2443–2446.
(9) Wang, X.; Seeman, N. C. *J. Am. Chem. Soc.* **2007**, *129*, 8169–8176.
(10) Liu, H.; Chen, Y.; He, Y.; Ribbe, A. E.; Mao, C. *Angew. Chem., Int. Ed.* **2006**, *45*, 1942–1945.
(11) Chen, J.; Seeman, N. C. *Nature* **1991**, *350*, 631–633.
(12) Wang, Z. G.; Wilner, O. I.; Willner, I. *Nano Lett.* **2009**, *9*, 4098–4102.
(13) LaBean, T. H.; Yan, H.; Kopatsch, J.; et al. *J. Am. Chem. Soc.* **2000**, *122*, 1848–1860.
(14) Boer, D. R.; Kerckhoffs, J. M.; Parajo, Y.; Pascu, M.; Usón, I.; Lincoln, P.; Hannon, M. J.; Coll, M. *Angew. Chem., Int. Ed.* **2010**, *49*, 2336–2339.
(15) Li, Y.; Tseng, Y. D.; Kwon, S. Y.; D'Espaux, L.; Bunch, J. S.; McEuen, P. L.; Luo, D. *Nat. Mater.* **2004**, *3*, 38–42.
(16) Li, Y.; Cu, Y. T.; Luo, D. *Nat. Biotechnol.* **2005**, *23*, 885–889.
(17) Nakayama, S.; Yan, L.; Sintim, H. O. *J. Am. Chem. Soc.* **2008**, *130*, 12560–12561.
(18) Qiu, L. P.; Wu, Z. S.; Shen, G. L.; Yu, R. Q. *Anal. Chem.* **2011**, *83*, 3050–3057.
(19) Yan, L.; Nakayama, S.; Yitbarek, S.; Greenfield, I.; Sintim, H. O. *Chem. Commun.* **2011**, *47*, 200–202.
(20) Gerasimova, Y. V.; Peck, S.; Kolpashchikov, D. M. *Chem. Commun.* **2010**, *46*, 8761–8763.
(21) Kong, R. M.; Zhang, X. B.; Zhang, L. L.; Huang, Y.; Lu, D. Q.; Tan, W.; Shen, G. L.; Yu, R. Q. *Anal. Chem.* **2011**, *83*, 14–17.
(22) Mokany, E.; Bone, S. M.; Young, P. E.; Doan, T. B.; Todd, A. V. *J. Am. Chem. Soc.* **2010**, *132*, 1051–1059.
(23) Labib, M.; Ghobadloo, S. M.; Khan, N.; Kolpashchikov, D. M.; Berezovski, M. V. *Anal. Chem.* **2013**, *85*, 9422–9427.
(24) Zhang, H.; Li, F.; Dever, B.; Wang, C.; Li, X.-F.; Le, X. C. *Angew. Chem., Int. Ed.* **2013**, *52*, 10698–10705.
(25) Zhang, H.; Li, X.-F.; Le, X. C. *Anal. Chem.* **2012**, *84*, 877–884.
(26) Zhang, H.; Li, F.; Dever, B.; Li, X.-F.; Le, X. C. *Chem. Rev.* **2013**, *113*, 2812–2841.
(27) Li, F.; Zhang, H.; Wang, Z.; Li, X.; Li, X.-F.; Le, X. C. *J. Am. Chem. Soc.* **2013**, *135*, 2443–2446.
(28) Li, F.; Lin, Y.; Le, X. C. *Anal. Chem.* **2013**, *85*, 10835–10841.
(29) Zhang, H.; Li, F.; Li, X.-F.; Le, X. C. *Methods* **2013**, *64*, 322–330.
(30) Li, F.; Zhang, H.; Lai, C.; Li, X.-F.; Le, X. C. *Angew. Chem., Int. Ed.* **2012**, *51*, 9317–9320.

(31) Li, J.; Zhong, X.; Zhang, H.; Le, X. C.; Zhu, J. J. *Anal. Chem.* **2012**, *84*, 5170−5174.